WATER RESOURCES RESEARCH, VOL. 27, NO. 12, PAGES 3225–3235, DECEMBER 1991

# Application of Energy Concepts to Groundwater Flow: Time Step Control and Integrated Sensitivity Analysis

BRYAN W. KARNEY AND ASITHA SENEVIRATNE[1]

*Department of Civil Engineering, University of Toronto, Toronto, Ontario, Canada*

When fluid passes into or out of an aquifer, work is done at the boundaries which is used partly to change the internal energy of the system and partly to overcome resistance to flow. For a saturated medium, the change in internal energy is further partitioned into two terms, the strain energy stored in the elastic soil matrix and the strain energy stored in the pore water due to compression. A technique is developed in this paper which interprets the dynamic behavior of an aquifer in terms of its energy transformations. The central feature of this approach is the quantification of the physical processes into individual energy and work parameters which together characterize the response of an entire aquifer to a given set of excitations. By this means, the rate of change of strain energy is shown to be a natural index of the unsteadiness of a system, an insight which leads to an adaptive algorithm for adjusting the time step of a transient groundwater flow model. Further, the energy approach is used to assess differential compaction in a heterogeneous aquifer, thereby providing a basis for efficient computation and for rational acquisition of compressibility data.

## INTRODUCTION

Groundwater-related problems often require considerable effort for both analysis and collection of data. Although progress has been made, there is need for further understanding of how a porous medium responds to various development schemes as well as for computationally efficient modeling techniques. This paper continues the search for better analysis techniques by describing transient flow conditions in a porous medium in terms of composite energy functions. The underlying concept is simple: When equilibrium flow conditions are disturbed, changes to a system's energy are partitioned among several components, the relative magnitude of which indicates the dominance of the different events in a system. Unlike the traditional approach of focusing attention on conditions at a finite set of points, the energy method provides an integrated view of the transient response of the entire system.

One significant advantage of the energy method is the ease with which the state of a system can be assessed. As subsequent developments show, the rate of change of strain energy is an excellent index of the unsteadiness of a system. The basic idea is that systems undergoing rapid changes require smaller time increments than systems near steady state. The new approach adjusts the time step based on the ratio of the rate of energy dissipation in a region to the rate of change of strain energy. This nondimensional procedure permits dynamic adjustment of the time step in any domain and can considerably improve execution times.

In this preliminary paper, the energy concepts are developed from first principles and applied to a one-dimensional flow situation only. However, direct extension of the energy method to higher dimensions is possible and it is in these more complex problems that the energy approach has the greatest potential as an interpretive tool.

[1]Now at Jacques Whitford Environment Limited, Fredricton, New Brunswick, Canada.



Paper number 91WR01909.
0043-1397/91/91WR-01909$05.00

## THE ENERGY METHOD

In the following sections, a general approach is developed from first principles and then by mathematical manipulation of the traditional governing equations. To place these developments in perspective, a brief review of energy principles in groundwater applications is presented.

### *Historical Background*

In his pioneering article, "The Theory of Groundwater Motion," *Hubbert* [1940] applied energy principles to the problem of describing groundwater motion. Hubbert introduced the "fluid potential" as the work required to displace a unit mass of fluid from a reference state to a new state. The fluid potential $\Phi$ for a unit control mass of the fluid was then expressed as

$$\Phi = gz - p_0V_0 + \int_V^{V_0} pdV + pV + \frac{v^2}{2} \qquad (1)$$

in which $g$ is the acceleration due to gravity, $z$ is the elevation above the reference state, $p$ is the fluid pressure, $v$ is the fluid velocity, $V$ is the specific fluid volume, and the subscript 0 indicates conditions at the reference state. Collectively, $gz$ is the gravitational potential energy and $v^2/2$ is the kinetic energy per unit mass. Two distinct work components contribute to the flow: the $\int_V^{V_0} pdV$ term is associated with the compressibility of the porous medium and the so-called "flow work" " is represented by $pV - p_0V_0$.

When integrated by parts, the definite integral in (1) becomes

$$\int_V^{V_0} p\ dV = p_0V_0 - pV + \int_{p_0}^{p} V\ dp.$$

This relation transforms (1) into the total hydraulic energy potential for a barotropic fluid:

$$\Phi = gz + \int_{p_0}^{p} V\ dp + \frac{v^2}{2}. \qquad (2)$$

Several references [e.g., *Freeze and Cherry*, 1979; *Bear*, 1979] use (2) to motivate Bernoulli's equation and Darcy's law. Yet, from an energy point of view, this second equation obscures the role of compressibility. Part of the $\int_{p0}^{p} V\,dp$ term is involved with flow processes that are present whenever flow occurs, even if the flow is steady; the other part is associated with compressibility effects that are most significant under transient conditions.

The physical insights that are possible using energy concepts in porous media flows have advanced little since Hubbert's work. This is unfortunate since energy arguments are not only useful in deriving and motivating relationships, they are also an aid in interpreting many kinds of phenomena. In what follows, the physical insights are developed in parallel with what appears to be a rather arbitrary set of mathematical manipulations. This parallel derivation is essential. The physical approach develops insight, while the mathematical derivations show the connection between the traditional governing equations and the integrated energy expressions. In this way, links are forged not only to Hubbert's original work but also to the mathematical literature. In fact, the expressions that follow can be interpreted as a special case of *Gurtin*'s [1964] energy functional. Gurtin's approach was originally derived for the heat conduction problem and is difficult to apply to complex domains. A more direct approach to the energy equation for flow in porous media is presented here.

### *Strain Energy Density of a Saturated Elastic Porous Medium*

When a fluid flows through a saturated elastic soil matrix, the net work done at the boundary of a control volume is partitioned among three events: the elastic compression of the soil matrix, the elastic compression of the fluid and the energy dissipation due to friction. Expressions for the first two of these terms are derived from first principles in this section. Note, however, that other energy terms also must be accounted for in more complex media. For example, in an unsaturated porous medium, energy terms must account for surface tension effects and potential energy due to gravity.

Consider a saturated soil volume $V_b$, initially in equilibrium, compressed by an infinitesimal volume change $\partial V_b$ under an effective normal stress $\sigma'$ ($kN/m^2$). The change in strain energy of the soil matrix $\partial E_{\text{soil}}$ is equal to the work of compression $\sigma' \partial V_b$; that is,

$$\partial E_{\text{soil}} = \sigma' \partial V_b. \tag{3}$$

The constant coefficient of compressibility ($\alpha$) of the soil under undrained conditions may be defined as

$$\alpha = -\frac{1}{V_b}\frac{\partial V_b}{\partial \sigma'} \tag{4}$$

Eliminating $\partial V_b$ from (3) and (4) gives

$$\partial E_{\text{soil}} = -\tfrac{1}{2}\alpha V_b \partial[(\sigma')^2]. \tag{5}$$

For a constant overburden stress, the change in pore water pressure $\partial p$ is equal to the negative of the change in effective stress $\partial \sigma'$. Since $p = (h - z)\,\rho g$, the change of effective stress can also be written as

$$\partial \sigma' = -\partial[(h + z)\rho g]. \tag{6}$$

Hence, $\sigma' = h\rho g + C_1$ in which $C_1$ is a constant. By selecting a datum appropriately, $C_1$ can be made zero. Substituting for $\sigma' = h\rho g$ in (5) gives

$$\partial E_{\text{soil}} = -\tfrac{1}{2}\alpha V_b \partial[(h\rho g)^2]. \tag{7}$$

The strain energy density of the soil matrix $\zeta_{\text{soil}}$ may be defined as $E_{\text{soil}}/V_b$. With this substitution, the time rate of change of the strain energy density of the soil becomes

$$\frac{\partial \zeta_{\text{soil}}}{\partial t} = \frac{1}{2}\alpha \frac{\partial[\rho^2 g^2 h^2]}{\partial t}. \tag{8}$$

As a practical aside, it should be noted that the magnitude of $E_{\text{soil}}$ depends on the selection of the piezometric head datum. However, since only changes in strain energy are usually of interest, the piezometric drawdown $(h - h_0)$ can replace $h$ in the computation of the various energy expressions. As a result, $E_{\text{soil}}$ is initially zero and any change is about this initial condition. This substitution of drawdowns for piezometric heads simplifies the interpretation of the energy equation in the same way that energy expressions in mechanical systems are simplified by measuring displacements with respect to equilibrium.

### *Strain Energy Density of Water*

If the saturated soil volume $V_b$ has a porosity $n$, the volume of pore water is $V_w = nV_b$. The coefficient of compressibility $\beta$ of water may be defined as,

$$\beta = -\frac{1}{V_w}\frac{\partial V_w}{\partial p}. \tag{9}$$

Following a derivation parallel to that shown for the soil energy term, the rate of change of the strain energy density in the water can be expressed as

$$\frac{\partial \zeta_{\text{water}}}{\partial t} = \frac{1}{2} n\beta \frac{\partial[\rho^2 g^2 h^2]}{\partial t}. \tag{10}$$

## Energy Relations: An Overview

The laws of thermodynamics stipulate that the equilibrium state of a system is altered only if heat and/or work are exchanged with the system's environment. In addition, the laws imply that a different equilibrium state is associated with each value of a system's energy; thus, if no heat or work are done on the system, the equilibrium state cannot be changed. When written for mechanical energy in a saturated porous media, conservation of energy requires that the net work done on a system $dW$ be partitioned between changes in internal energy $dE$ and frictional dissipation (conversion to heat) in the system. Thus,

$$dW = dE + dD \tag{11}$$

in which $dD$ is the mechanical energy dissipated to overcome friction. Rewriting (11) as a rate relation and recognizing that

$$\frac{dE}{dt} = \frac{\zeta_{\text{soil}}}{dt} + \frac{\zeta_{\text{water}}}{dt} = \frac{1}{2}[\alpha + n\beta]\frac{\partial[\rho^2 g^2 h^2]}{\partial t} \tag{12}$$

produces

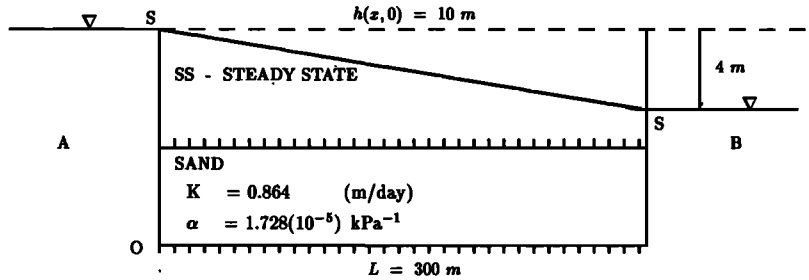


Fig. 1. Aquifer bounded by two constant head reservoirs: flow case 1.

$$\frac{dW}{dt} = \frac{\zeta_{\text{soil}}}{dt} + \frac{\zeta_{\text{water}}}{dt} + \frac{dD}{dt}. \tag{13}$$

Equation (13) is a generic equation for the energy in a saturated soil volume. The next section provides an alternative interpretation of the energy equation which shows its relation to the usual equations governing flow in a porous medium. In particular, the energy equation is derived by manipulating the usual continuity equation and Darcy's law in a one-dimensional domain.

## The One-Dimensional Energy Equation

The energy equation is now developed for one-dimensional flow in a saturated heterogeneous confined aquifer of constant thickness. The equation of continuity for a control volume of length $\delta x$, unit width, and constant thickness $\beta$ can be written as [*Bear*, 1979],

$$\frac{\partial(\rho v_x)}{\partial x} + \frac{\partial(n\rho)}{\partial t} = 0. \tag{14}$$

Further, Darcy's law may be expressed as,

$$v_x + K_x \frac{\partial h}{\partial x} = 0. \tag{15}$$

where $h$ is the piezometric head, $v_x$ the Darcy velocity, $n$ is the average porosity, $K_x$ is the hydraulic conductivity, $\rho$ is the fluid density and $x$ and $t$ are the space and time variables respectively.

Following a procedure similar to *Karney* [1990], (14) can be multiplied by $h$ and (15) by $\rho v_x/K_x$ and the two equations summed to produce

$$h\frac{\partial(\rho v_x)}{\partial x} + \rho v_x \frac{\partial h}{\partial x} + \rho\frac{v_x^2}{K_x} + h\frac{\partial(n\rho)}{\partial t} = 0. \tag{16}$$

This equation can be multiplied by $g\,dx$ and integrated with respect to $x$ over a length $L$. The result is

$$g[\rho v_x h]_{x=0}^{x=L} + \int_{x=0}^{x=L} \rho g \frac{v_x^2}{K_x}\,dx + \int_{x=0}^{x=L} gh\frac{\partial(n\rho)}{\partial t}\,dx = 0. \tag{17}$$

In addition, *Bear* [1979] shows that

$$\frac{\partial(n\rho)}{\partial t} = \rho^2 g[\alpha + n\beta]\frac{\partial h}{\partial t}. \tag{18}$$

Using this relation in (17) produces

$$\int_{x=0}^{x=L} \rho g \frac{v_x^2}{K_x}\,dx + \frac{1}{2}\int_{x=0}^{x=L} [\alpha + n\beta]\rho^2 g^2 \frac{\partial[h^2]}{\partial t}\,dx = -g[\rho v_x h]_{x=0}^{x=L}. \tag{19}$$

This equation summarizes the various energy transformations taking place in a saturated, one-dimensional, confined aquifer of constant thickness; in the SI system of units, each term in the equation has dimensions of joules per second or watts. Thus, (19) corresponds to the general energy equation (13). The first term in (19) represents the frictional dissipation. The second term represents the change in internal energy due to compression of both the soil matrix and pore water (compare with (8) and (10)). Finally, the right-hand side of (19) represents the net work at the domain boundaries. Clearly, the sum of the energy transformations within a control volume is equal to the net work at the boundaries. This observation is used subsequently to characterize flow conditions in a porous medium.

Note that (19) allows a natural classification of flow regimes:

1. When the flow is steady, the rate of change of internal energy of the system is zero; there is equilibrium between the flow work and mechanical energy dissipation.
2. If the rate of dissipation is dominant compared to the rate of change of internal energy, then the compressibility effects of the system are insignificant. The changes in such a system are "quasi-steady" and allow larger time steps to be used by the flow model, thereby improving the computational efficiency.
3. If the internal energy term is dominant compared to the dissipation, then the compressibility effects of the system are significant and the system's response should be treated as fully transient.

## Partitioning of Energy in Aquifers

In this section, the energy approach is illustrated by considering the transient behavior of several aquifers subjected to time-dependent boundary conditions. Initially, the solution to two simple flow problems is discussed and the energy approach is contrasted to the more traditional piezometric head summaries. Following this, a more complex time-dependent boundary condition is considered.

Figure 1 shows a one-dimensional saturated confined aquifer bounded by two constant head reservoirs. The equation which describes the transient flow in this domain is usually written as

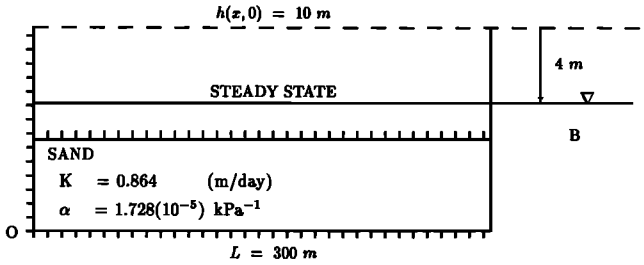


Fig. 2. Aquifer bounded by constant head and no-flow boundaries: flow case 2.

$$\frac{\partial\left(T\dfrac{\partial h}{\partial x}\right)}{\partial x} = S\frac{\partial h}{\partial t} \tag{20}$$

in which $T$ is the transmissivity and $S$ is the storage coefficient of the aquifer. In this example, the aquifer material is assumed to be homogeneous sand with a hydraulic conductivity of $10^{-5}$ m/s (0.864 m/day) and a compressibility of $1.728 \times 10^{-5}$ kPa$^{-1}$. The compressibility of water is $7.7 \times 10^{-7}$ kPa$^{-1}$. The response of this basic system is considered for two different excitations:

1. For flow case 1, the water level in both reservoirs and the piezometric head distribution in the aquifer are both initially set at 10 m. At the instant the simulation begins, the water level in reservoir B suddenly drops by 4 m. Thus, the initial and boundary conditions are respectively, $h(0, t) = 10.0$ m, $h(L, t) = 6.0$ m and $h(x, 0) = 10.0$ m.

2. For flow case 2, the same aquifer is bounded by only one constant head boundary and a no-flow boundary (Figure 2). The initial and boundary conditions are respectively, $\partial h(0, t)/\partial x = 0$, $h(L, t) = 6.0$ m and $h(x, 0) = 10.0$ m.

In both cases, the transient drawdown in the aquifer is monitored at distances 50 m and 150 m from the origin $O$. Once the flow equation is solved, the computed piezometric head $h$ and the Darcy velocity $v$ can be substituted in the energy equation to obtain the magnitudes of the energy components.

## Verification of the Flow Model

Because of their simplicity, the head distribution obtained using a Galerkin's finite element program [e.g., *Huyakorn and Pinder*, 1983; *Wang and Anderson*, 1982; *Pinder and Gray*, 1977] can be compared with a closed form solution for the first two flow cases.

For flow case 1, the generalized Fourier series solution is [*Haberman*, 1987]

$$h(x, t) = h_s(x) + \sum_{n=1}^{\infty} a_n \exp\left\{-\left[\frac{n\pi}{L}\right]^2 \kappa t\right\} \sin\frac{n\pi x}{L} \tag{21}$$

in which $\kappa = T/S$, $h_s(x)$ is the steady state solution and $a_n$ are coefficients. Specifically, $h_s(x)$ is given by

$$h_s(x) = h(L, t) + \frac{[h(0, t) - h(L, t)]x}{L} \tag{22}$$

while $a_n$ is obtained from

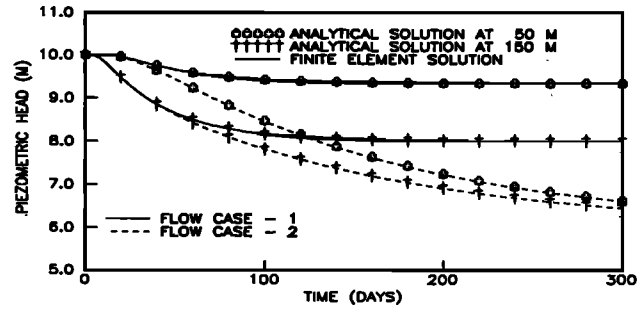


Fig. 3. Effect of different boundary conditions on aquifer response.

$$a_n = \frac{2}{L}\int_{x=0}^{x=L} [h(x, 0) - h_s(x)] \sin\frac{n\pi x}{L}\, dx. \tag{23}$$

The piezometric head distribution calculated from the finite element solution is compared with the sum of the first 150 terms of the Fourier series solution in Figure 3. Very good agreement is observed.

The generalized Fourier series solution for flow case 2 is [*Haberman*, 1987],

$$h(x, t) = h_s(x) + \sum_{n=1}^{\infty} a_n \exp\left\{-\left[\frac{(2n-1)\pi}{2L}\right]^2 \kappa t\right\} \cdot \sin\frac{(2n-1)\pi x}{2L}. \tag{24}$$

In this case, $h_s(x) = h(L, t)$ while $a_n$ is given by

$$a_n = \frac{2}{L}\int_{x=0}^{x=L} [h(0, t) - h_s(x)] \sin\frac{(2n-1)\pi x}{2L}\, dx. \tag{25}$$

The analytical solution generated by summing 150 terms of the Fourier series is compared with the finite element solution in Figure 3. Again there is good agreement between the two solutions.

The general energy equation (19) was also verified using the finite element code. This was done by comparing the sum of the individual energy terms on the left-hand side of the energy equation with the computed work term on the right side at each time step. It was found that left and right sides of (19) agreed to 3 decimal places for both flow cases tested. With these preliminaries completed, the finite element code can be used to illustrate the energy approach.

## Energy Interpretation

The energy response of the aquifer in flow case 1 is depicted in Figures 4–6. Figure 4 depicts the piezometric head distribution at specified locations while Figures 5 and 6 show the relative magnitudes of the different energy components. The rapid drawdown in head at one boundary results in large piezometric head gradients, thereby inducing high velocities and strain energies within the system. Figure 5 shows that the transient response of the system gradually diminishes and approaches steady state around 100 days. At this time, the rate of change of strain energy of the soil

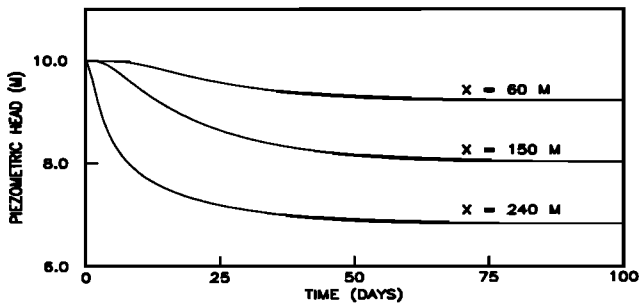


Fig. 4. Piezometric head distribution for flow case 1.

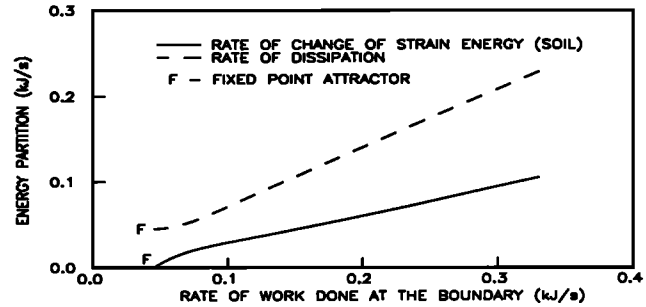


Fig. 6. Phase plot of energy partitioning for flow case 1.

matrix tends to zero implying that compressibility effects of the porous matrix are not governing the flow. Hence, all of the work at the boundaries is used to overcome frictional dissipation.

Figure 6 is a phase plot which represents the same energy transformations for flow case 1. On the phase plot, the response of the whole system at a particular time is represented by a point. When the system changes the point traces a path on the phase plot. Figure 6 reveals that a large fraction of the work at the boundaries is transformed into frictional dissipation and shows that, with time, the system converges to the new steady state (point F). At steady state, the change in strain energy is zero and the work done on the porous volume is entirely used to overcome friction. Point F is called a fixed point attractor.

Note that in Figure 3 the aquifer with the two constant head boundaries exhibits a faster response than the aquifer with one no-flow boundary. In both cases, there is a rapid drawdown in head at one boundary and work interactions gradually bring the system to a steady state. However, in the first case, both head boundaries bring the system into steady state, while in the second case the work done at the no-flow boundary is zero. Hence, only one boundary influences the change in the system and steady state will be reached at a slower rate than in the first case.

The energy terms spatially integrate the response of any specified subdomain in an aquifer. Conventional summaries, such as those shown in Figure 4, depict the piezometric head variation at specific locations and do not reveal the response of the aquifer as a whole. Such single point assessments can be misleading because the rate of change of flow parameters varies from point to point. For example, in a highly compressible medium such as clay, steady state conditions may prevail at some points in the domain, while others may still be in a transient state. In the energy approach, flow phenomena are integrated over any part of the domain in a way that enables a comparison of individual physical effects. Another application of this insight is when assessing the importance of compressibility effects in an elastic aquifer. If work at the control surface is used primarily to overcome frictional dissipation, the strain energy effects of the elastic matrix are insignificant. This implies that the compressibility effects are unimportant and that a more efficient "quasi-steady state" model can be used with little loss of accuracy.

## TIME-DEPENDENT BOUNDARY CONDITIONS

In this section, energy transformations in an aquifer due to a time-dependent boundary condition are analyzed. The aquifer depicted in Figure 1 is excited by the variable boundary condition shown in the upper portion of Figure 7. The resulting piezometric head distributions at specified locations are shown in the lower portion of Figure 7. The system reaches equilibrium around 100 days and remains steady until 200 days. On the day 200, a "flood wave" increases the boundary head at reservoir B to 8 m and remains constant for 20 days. The sudden increase in the boundary head recharges the depleted (compressed) aquifer after which the head drops to 2 m again.

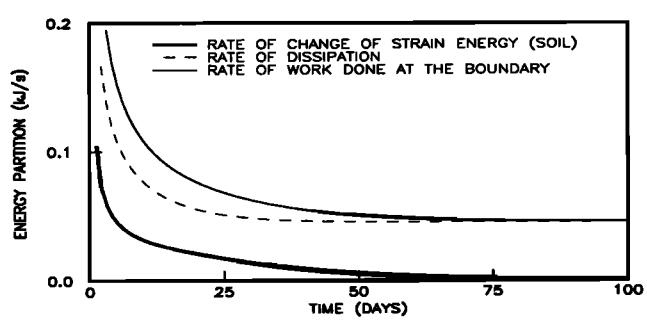


Fig. 5. Energy partitioning for flow case 1.

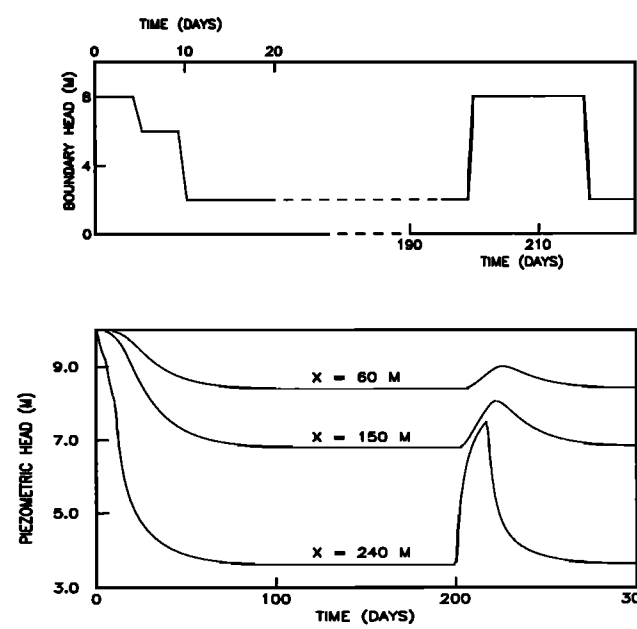


Fig. 7. Head distribution and the time-dependent boundary.

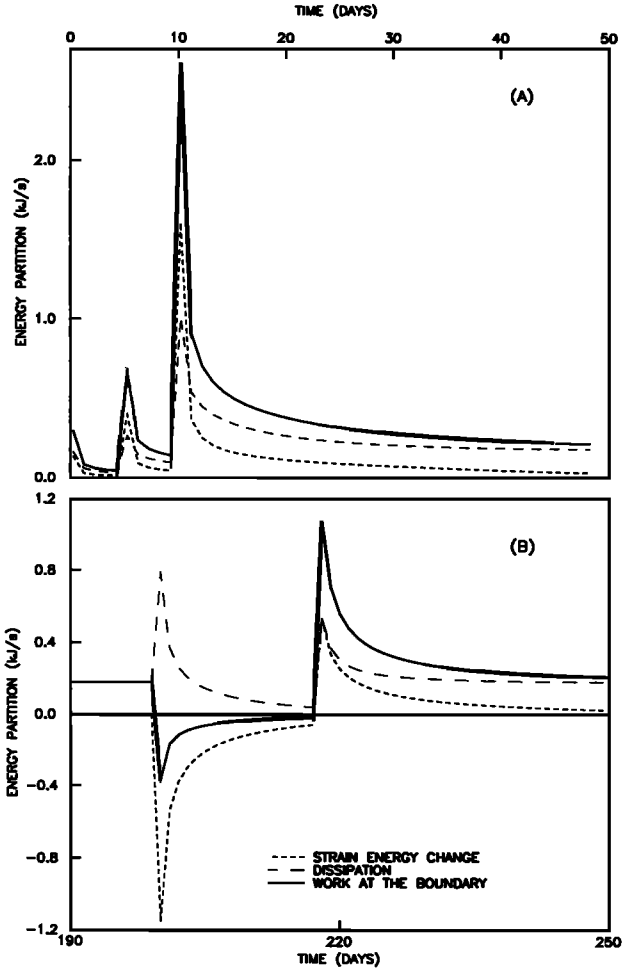


Fig. 8. Energy partitioning for the time-dependent boundary.

The energy relations for this case are shown in Figure 8. Figure 8*a* shows the energy partitioning for the first 50 days of simulation. The three peaks depict the increase in the rate of strain energy that occurs when the boundary head drops during the first period of excitation (1–20 days). The system reaches steady state around 50 days and remains steady until 200 days.

The recharge which occurs in the system between 200 and 220 days "expands" the compressed aquifer, reverses the sign of the rate of change of strain energy, and causes a discontinuity in the energy plot shown in Figure 8*b*. The nonequilibrium conditions due to the rapid drop in the reservoir B create a hydraulic head gradient toward reservoir B which discharges water from the aquifer, compressing the system. The rate of change of strain energy changes sign again as shown in the discontinuity in Figure 8. Beyond 220 days, the reservoir head remains constant at 2 m and the system gradually approaches steady state.

## Adaptive Time Step Control

The examples illustrate how the state of an aquifer can be interpreted with the energy approach. One application of the energy method is immediately suggested by this insight: to use the energy method for controlling or adjusting the time step in a transient algorithm. This procedure is described in this section.

Many different adaptive strategies have been used in both groundwater and petroleum engineering applications. Automatic time selector procedures for oil reservoir modeling were developed by *Jensen* [1980] and *Mehra et al.* [1982]. *Sammon and Rubin* [1983] developed an error-driven time step selection scheme based on techniques developed by *Lindberg* [1977]. In this paper, the time step is adjusted by assessing the dynamic energy response of the system.

When an aquifer is excited, either by changing boundary conditions or by external forcing functions such as groundwater pumping, the system undergoes transient conditions before reaching a new steady state. Such unsteady conditions are reflected by the rate of change of the strain energy of a porous medium. As the system approaches the new steady state, changes in the strain energy gradually diminish. The changing strain energy can be described by the initial value problem,

$$\frac{dE}{dt} = e(t) \tag{26}$$

where $e(t)$ is the rate of change of strain energy at time $t$ and $E(t)$ is the strain energy stored in the porous matrix at $t$. The initial condition $E(t = 0) = E_0$ is usually assumed to be zero since only changes in the strain energy are important.

To develop an adaptive method of choosing the time step, let the minimum time increment used during periods of rapid excitation in a time-stepping algorithm be $\delta t_{\text{base}}$. This value is the time step which is adopted by default if adaptive time control is not used. However, under less severe transient conditions, the time step can be increased to $\delta t_{\text{adapt}} > \delta t_{\text{base}}$. Using a first-order approximation of Taylor's series to express (26) in discrete form gives

$$E(t + \delta t_{\text{base}}) - E(t) = e(t)\delta t_{\text{base}}. \tag{27}$$

If the time is increased to $\delta t_{\text{adapt}}$, an analogous relation applies:

$$E(t + \delta t_{\text{adapt}}) - E(t) = e(t)\delta t_{\text{adapt}}. \tag{28}$$

Subtracting (27) from (28) and solving for $\delta t_{\text{adapt}}$ gives

$$\delta t_{\text{adapt}} = \frac{E(t + \delta t_{\text{adapt}}) - E(t + \delta t_{\text{base}})}{e(t)} + \delta t_{\text{base}}. \tag{29}$$

If the rate of change of strain energy $e(t)$ is known, (29) allows $\delta t_{\text{adapt}}$ to be chosen for a specified discrepancy in internal energy value between the two predictions. In effect, the rate of change of internal energy $e(t)$ becomes an index of how quickly the system is responding while the deviation $|E(t + \delta t_{\text{adapt}}) - E(t + \delta t_{\text{base}})|$ indicates how much the energy state of the system is permitted to change. The relation is logical since the internal energy of a system $e(t)$ only changes under transient conditions; as steady state is approached, the permissible time step increases as the value of $e(t)$ decreases. The magnitude of the deviation determines how important transient effects are to a given system and, hence, how large a time step can be used for a given rate of change $e(t)$.

Note that the selection of an appropriate value of the deviation in (29) depends not only on the dynamics of the porous medium, but also on its size and dimensions. Thus, it

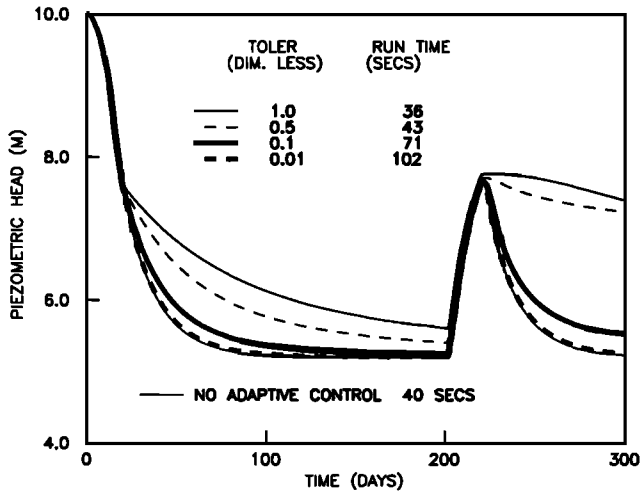


Fig. 9. Accuracy of the solution for different levels of tolerance: flow case 1.

appears to be difficult to select an optimal value for the deviation without a prior knowledge of the dynamics of the system. Fortunately, however, it is simple to scale the deviation to produce a nondimensional tolerance TOLER. This is accomplished by dividing the deviation by the time-averaged dissipation during the previous time step $\delta t_p$. That is, the product $\delta t_p \int (v^2/K)\, dx$ replaces the deviation in (29) to produce

$$\delta t_{\text{adapt}} = \delta t_{\text{base}} + \delta t_p \text{ TOLER} \frac{\int \frac{v^2}{K} dx}{e(t)}. \quad (30)$$

It is the physics of the flow problem that justifies this choice of scaling factor. Under highly transient conditions, a large fraction of the work interactions is used to change the internal energy of the system. In this case, the dissipation is relatively low, the change in internal energy high and the resulting time step small. However, as the system approaches equilibrium the importance of the strain energy term diminishes and the work is used primarily to overcome frictional dissipation. The result is a high ratio of the rate of dissipation to the change in internal energy and a large time step. (In practice, it is required to limit the maximum time step to some multiple of the base step.) Note that the ratio of term in (30) is well-behaved in that the internal energy cannot change unless there is flow and, thus, dissipation. The only way both terms can be zero is if there is no flow (trivial solution).

In summary, the ratio dissipation/rate of strain energy change is a natural index of the "state of the system." The adaptive time step $\delta t_{\text{adapt}}$ is evaluated by the system at each time level based on (30). For a specified tolerance, the adaptive time step is inversely related to the rate of change of the strain energy. When the system approaches steady state, the adaptive algorithm computes larger time steps because of the diminishing magnitude of the rate of change of strain energy. The piezometric head at any point is not to be used as a controlling parameter, since it represents only a specific point and does not represent the entire system.

To illustrate the use of adaptive time control, consider again the flow situation described in Figure 7. Figure 9 depicts the piezometric head response at a hypothetical observation well 150 m from the origin, for different values of TOLER. It is observed that the accuracy of the adaptive solution improves when the tolerance is tightened. When TOLER = 0.01, the resulting piezometric head response is very close to the solution without adaptive control.

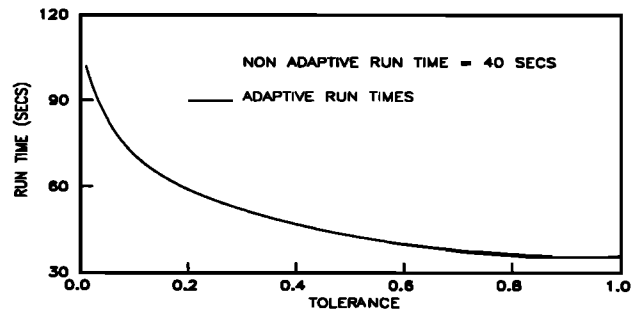


Fig. 10. Run times for different degrees of tolerance.

Figure 10 shows the execution times when the system is simulated using different values of TOLER on a 386 PC (16-MHz clock and 30387 math coprocessor). The execution time includes both the computation and the reading of the input data for a simulation time of 300 days. For the case with no adaptive control (base solution), the computational time was 40 s. The "best fit" adaptive solution took longer to run (102 s). The reason is obvious: The integration associated with the energy principle added a computational burden to the program that was not made up for by the longer time step. However, if energy summaries are computed for both runs, or if longer periods of simulation are used, the run time for the adaptive procedure is often reduced compared to the nonadaptive solution.

Flow case 1 is simulated for different time horizons using both the base solutions and an adaptive solution with a tolerance of $10^{-2}$. Figure 11 depicts the run times in seconds versus the simulation period in years. When the time horizon increases, the gain in computation efficiency also increases when adaptive procedures are used, and it is in these problems that the adaptive time-stepping procedures become more relevant to improve the run times.

## Compressibility Effects in Heterogeneous Media

When a heterogeneous aquifer is excited by an external force such as pumping, different regions of the aquifer may exhibit different degrees of compression. The strain energy of a porous soil is a function of both the pressure head and

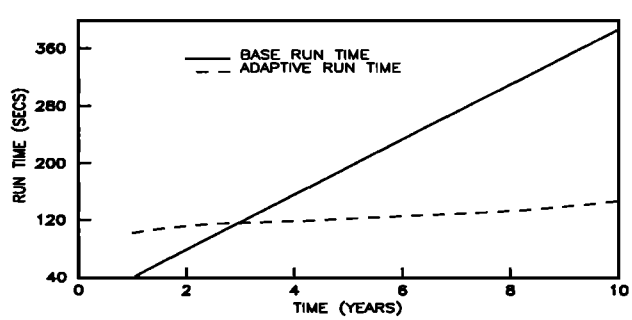


Fig. 11. Computational times with and without adaptive control.

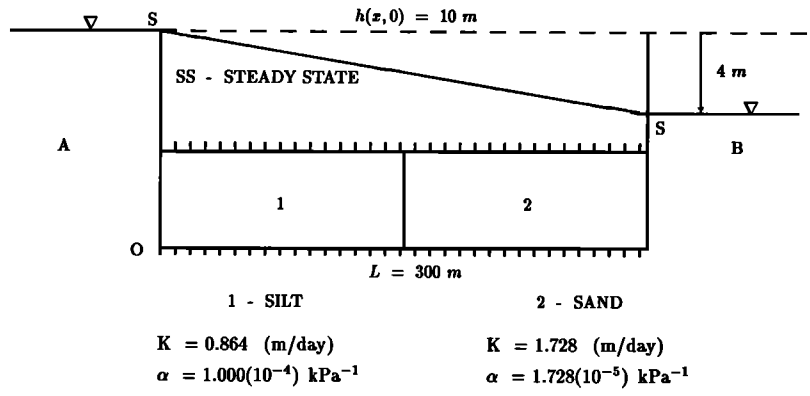


Fig. 12. Aquifer with heterogeneous material: flow case 1.

the compressibility of that medium, and can be used to assess the degree of compaction of the different materials in the aquifer.

The application of the strain energy concept is illustrated through the following examples. Flow case 1 is analyzed under two different soil conditions. In the first instance, the aquifer material is homogeneous sand while in the second the aquifer material consists of sand and silt as shown in Figure 12. The first 150-m region contains silt and the second region contains sand. Silt is assumed to have a hydraulic conductivity of 0.864 m/day and a compressibility of $10^{-4}$ $kPa^{-1}$ and the properties of sand are the same as previously reported. Figure 13 depicts the piezometric head variation at the observation well located at 180 m from the origin $O$.

The strain energies of the different soil layers are plotted against time in Figure 14. For the homogeneous case, portion 2 exhibits a much higher strain energy storage (≈5 kJ) compared to portion 1 (≈1 kJ). This is expected since portion 2 is close to the falling head boundary. In the heterogeneous case, sand shows a higher energy up to about 260 days. Hence, the sand layer compacts more than the silt layer during this period even though the silt has a higher compressibility. However, beyond 300 days, the silt is compressed more than the sand. The homogeneous case reaches steady state in close to 100 days while flow conditions are not steady in the heterogeneous case even at 500 days. Beyond 100 days, compressibility effects in the homogeneous aquifer are insignificant, and the system may be modeled by using a steady state model. However, for the period up to 100 days the system needs full transient modeling.

Flow case 2 is also analyzed under identical soil conditions as in Figure 12 with the exception that the constant head reservoir A is replaced with an impermeable boundary. This means that the final steady state in flow case 2 is a 4-m head drop everywhere. The piezometric head distribution at a well 180 m from the origin is plotted in Figure 15. Figure 16 shows that the final strain energy in both soil layers becomes equal, indicating no long-term differential compaction between the regions 1 and 2 in the homogeneous case.

For the heterogeneous case, the sand showed a higher degree of compaction during the initial periods while silt compacted more after 200 days. The observed strain energies are higher than in flow case 1 due to its larger drawdown. Further, silt shows a higher degree of compression at steady state. When Figures 14 and 16 are compared, it is seen that under homogeneous soil conditions at steady state, flow case 2 results in no differential compaction between zones 1 and 2 while flow case 1 shows a substantial differential compaction. However, under heterogeneous conditions the reverse occurs and flow case 1 has a smaller compaction at steady state.

Such an analysis helps to determine the areas which may be severely affected by the falling water level of a river or due to pumping of groundwater. Further, it indicates the importance of compressibility effects in a flow domain and helps to determine whether the system requires steady state or transient simulation. This feature may be particularly important in the transient analysis of heterogeneous aquifers since such systems require large quantities of both hydraulic conductivity and compressibility data. The present trend in groundwater modeling is to extrapolate localized data ob-

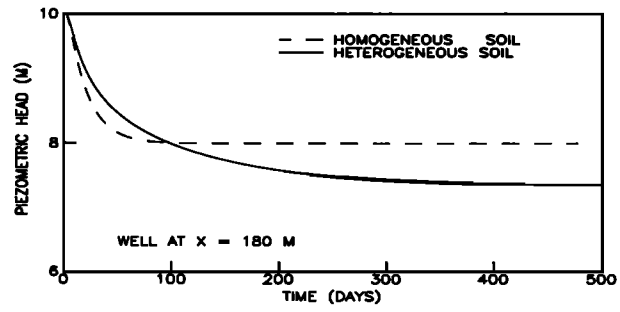


Fig. 13. Comparison of drawdown for the different soil conditions: flow case 1.

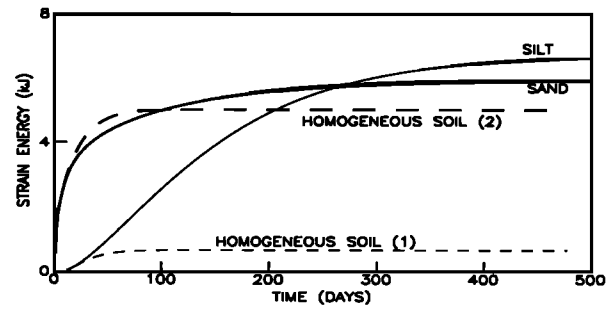


Fig. 14. Comparison of strain energy storage in different soil layers: flow case 1.

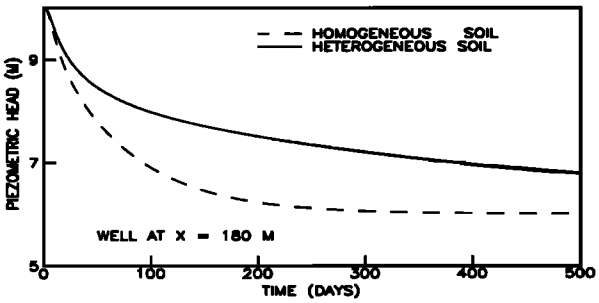


Fig. 15. Comparison of drawdown for the different soil conditions: flow case 2.

tained through pumping tests using standard techniques such as kriging. However, if the aquifer region of interest is insensitive to the detailed heterogeneities of the flow domain, more cost-effective acquisition of data may be possible. This concept is explored more completely in the following section.

## Integrated Sensitivity Analysis of Porous Media

Heterogeneities of the subsurface have always been difficult to model. However, when simulating such aquifers, the heterogeneities have been treated deterministically or stochastically depending on the extent of knowledge of the subsurface properties. In the absence of detailed data, it is better to understand the sensitivity of the given system to the unknown parameters. The traditional methods such as the influence coefficient method, the variational method and the method of sensitivity equations [*Yeh*, 1987] all compute the sensitivity of the aquifer at specified points on the flow domain. Such analyses are an inevitable starting point; however, the interpretation of these results for efficient data acquisition is both tedious and indirect. The approach developed in this paper indicates the sensitivity of an entire aquifer region or a subregion to a given parameter in contrast to the pointwise analysis of the traditional approaches. The technique is developed next from the basic expression for the rate of change of strain energy of a soil matrix with the assumption that the spatial variation in the fluid density $\rho$ is negligible. Hence, $\rho$ is considered a constant in the derivations to follow and is combined with $g$ to give $\gamma$, the unit weight of the fluid.

The rate of strain energy change of an aquifer reach of length $L_i$ is

$$E^i = \frac{1}{2}\alpha\gamma^2 \int_{x=0}^{x=L_i} \frac{\partial h^2}{\partial t}\,dx. \tag{31}$$

This equation can be rewritten as

$$E^i = (\alpha\gamma B)\frac{\gamma}{B}\int_{x=0}^{x=L_i} h\frac{\partial h}{\partial t}\,dx \tag{32}$$

in which $B$ is the saturated thickness. For a heterogeneous aquifer, the rates of strain energy change in the individual subdomains may be superimposed to give the total strain energy change in the aquifer to produce

$$E = \sum_{i=1}^{i=M} (\alpha_i\gamma B)\frac{\gamma}{B}\int_{x=0}^{x=L_i} h\frac{\partial h}{\partial t}\,dx. \tag{33}$$

Differentiating (32) with respect to the dimensionless quantity $\alpha_j\gamma B$ gives,

$$\frac{dE^i}{d(\alpha_j\gamma B)} = \left\{(\alpha_i\gamma^2)\int_{x=0}^{x=L_i}\left[h\frac{\partial\left[\dfrac{\partial h}{\partial(\alpha_j\gamma B)}\right]}{\partial t} + \frac{\partial h}{\partial t}\frac{\partial h}{\partial(\alpha_j\gamma B)}\right]dx + \frac{\gamma}{B}\frac{\partial[\alpha_i\gamma B]}{\partial[\alpha_j\gamma B]}\int_{x=0}^{x=L_i} h\frac{\partial h}{\partial t}\,dx\right\}$$

where

$$\frac{\partial[\alpha_i\gamma B]}{\partial[\alpha_j\gamma B]} = \delta_{ij} = 1 \qquad i = j$$
$$\frac{\partial[\alpha_i\gamma B]}{\partial[\alpha_j\gamma B]} = \delta_{ij} = 0 \qquad i \neq j \tag{34}$$

in which $\delta_{ij}$ is the Kronecker's delta function. The index $i$ ($i = 1, \cdots, M$) in (34) represents any generic region within the domain out of $M$ such different regions. Index $j$ ($j = 1, \cdots, M$) represents the region with respect to which the sensitivity analysis is carried out.

To compute $dE_i/d(\alpha_j\gamma B)$ in (34) it is also necessary to know $\partial h/\partial(\alpha_j\gamma B)$. Following a procedure recommended by *Yeh* [1987], the original flow problem is first differentiated with respect to $\alpha_j\gamma B$; then the transformed boundary value problem in which the dependent variable is $\partial h/\partial(\alpha_j\gamma B)$ is solved.

The flow equation (20) together with the specified head boundary and initial conditions can be written as

$$\frac{\partial\left[T\dfrac{\partial h}{\partial x}\right]}{\partial x} = B\rho g[\alpha_i + n\beta]\frac{\partial h}{\partial t} \tag{35}$$

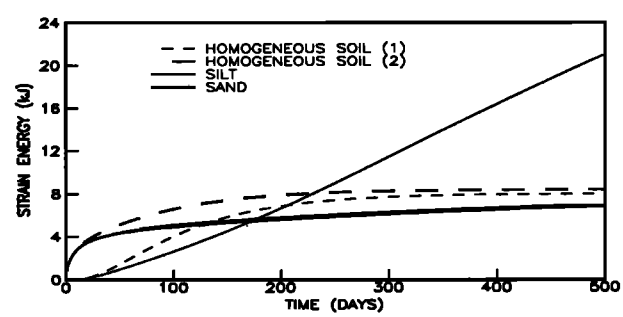


Fig. 16. Comparison of strain energy storage in different soil layers: flow case 2.

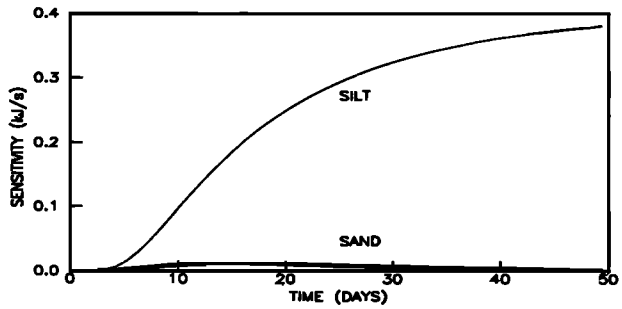


Fig. 17. Sensitivity of strain energies to bulk compressibility of silt.

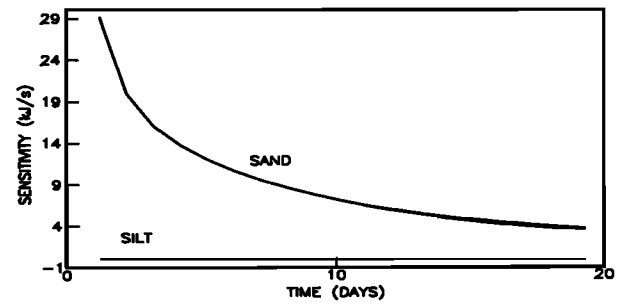


Fig. 18. Sensitivity of strain energies to bulk compressibility of sand.

and

$$h(0, t) = h(0)$$

$$h(L, t) = h(L) \quad \text{m} \tag{36}$$

$$h(x, 0) = h(x) \quad \text{m}$$

respectively. Differentiating (35) with respect to $\alpha_j \gamma B$,

$$\frac{\partial\left[T \dfrac{\partial h}{\partial(\alpha_j \gamma B)}\right]}{\partial x} = B\rho g[\alpha_i + n\beta] \frac{\partial\left[\dfrac{\partial h}{\partial(\alpha_j \gamma B)}\right]}{\partial t} + \frac{\partial(\alpha_i \gamma B)}{\partial(\alpha_j \gamma B)} \delta_{ij} \frac{\partial h}{\partial t} \tag{37}$$

The transformed boundary and initial conditions are respectively,

$$\frac{\partial h(0, t)}{\partial(\alpha \gamma B)} = 0 \tag{38}$$

$$\frac{\partial h(L, t)}{\partial(\alpha \gamma B)} = 0 \tag{39}$$

$$\frac{\partial h(x, 0)}{\partial(\alpha \gamma B)} = 0 \tag{40}$$

Equation (34) represents the marginal change in $E^i$ with respect to $\alpha_j \gamma B$. The relative magnitudes of $dE^i/d(\alpha_j \gamma B)$ indicate the influence of the bulk compressibility on different regions of the aquifer.

This sensitivity technique is illustrated for the system shown in Figure 12. The objective is to evaluate the sensitivity of the response of the sand layer to errors in the bulk compressibility data for either zone. Figure 17 depicts the sensitivity of the rate of strain energy change of the silt and sand zones to variations in the bulk compressibility of silt. The sensitivity of the rate of change of strain energy of the sand zone is much lower compared to the silt zone, for variations in silt compressibility. However, Figure 18 shows that sand is highly sensitive to variations in its own bulk compressibility. The indications of Figures 17 and 18 are verified in Figure 19 which displays the piezometric head at a well 240 m from the origin. The head distribution for the first 50 days is evaluated for different orders of magnitude of the bulk compressibility of both sand and silt. In the base case, silt has a compressibility of the order $10^{-4}$ m$^2$/kN while that of sand is of the order $10^{-5}$ m$^2$/kN. The compressibility of silt is first increased by an order of magnitude to $10^{-3}$ m$^2$/kN; the resulting percentage error of the piezometric head at the end of 50 days is approximately 3%. However, when the compressibility of sand is increased by an order of magnitude to $10^{-4}$ m$^2$/kN, the resulting percentage change increased to 22%.

The example shows that if drawdowns in the sand region are of importance, then compressibility data of the sand layer should be acquired with precision. Hence, the integrated sensitivity approach provides a basis to identify those regions which contribute mostly to the dynamic effects of a given study area of the aquifer.

## CONCLUSIONS

The concept of energy transformation presented in this paper provides a comprehensive way of analyzing dynamic aquifers. Central to the energy approach is its ability to evaluate the different physical phenomena occurring within an aquifer. For example, when water is pumped out of a confined aquifer, the porous matrix undergoes compression which is measured by the strain energy stored in the aquifer skeleton. Further, the rate of change of strain energy quantifies the transient nature of the aquifer. Integration of the individual processes within an aquifer into a representative single parameter makes it possible to compare the dominance of the flow phenomena in the aquifer. In summary, the energy method is an effective way of collapsing the dynamic behavior of aquifers into individual parameters describing the state of the system.

The contribution of this approach is its ability to assess and interpret flow conditions in a porous medium. For example, a model can select a variable time step based on

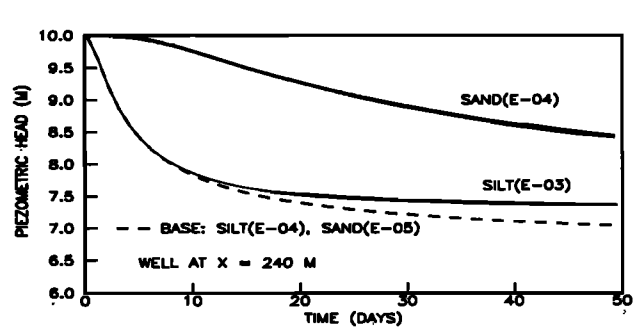


Fig. 19. Drawdown sensitivity to different compressibilities of sand and silt.

the rate of change of strain energy of the system. When the system undergoes rapid changes, the change in strain energy is also rapid and the time step small; as the system approaches steady state, the changes in strain energy gradually diminish and the size of the time step is increased. The adaptive control of the time step can improve the computational efficiency of the algorithm with a controllable loss of accuracy of the final solution. The computational efficiency of the adaptive algorithm increases with longer simulations. The adaptive control procedures are particularly suitable at a screening level when large numbers of simulations are required to narrow down the range of alternatives.

The energy method also evaluates the sensitivity of the flow model to the relative compressibilities of heterogeneous media under a given set of hydraulic conditions. This feature may be particularly important in identifying which areas may be affected due to aquifer development or due to a severe drawdown.

## NOTATION

$B$ constant saturated thickness.
$dD$ mechanical energy dissipated to overcome friction.
$dE$ change in internal energy.
$dW$ net work interactions at the control surface.
$E_{soil}$ strain energy stored in the soil matrix.
$E_{water}$ strain energy stored in the pore water.
$E$ strain energy of soil and water combined.
$e(t)$ rate of strain energy change in the soil matrix.
$g$ gravitational acceleration.
$h$ piezometric head.
$i$ a generic region with distinct aquifer properties.
$j$ region with respect to which the sensitivity analysis is done.
$K_x$ heterogeneous hydraulic conductivity.
$L$ length of the one-dimensional aquifer.
$M$ number of distinct aquifer regions.
$n$ porosity.
$p$ fluid pressure.
$p_0$ fluid pressure at the reference state.
$S$ storage coefficient.
$T$ heterogeneous transmissivity.
TOLER user-defined dimensionless tolerance.
$t$ time.
$V$ volume of fluid in a generic soil sample.
$V_0$ volume of fluid at the reference state.
$V_b$ bulk volume of the soil sample.
$V_w$ volume of water within the soil sample.
$v$ average fluid velocity within the soil pores.
$v_x$ flow velocity in the $x$ direction.
$x$ space dimension.
$z$ datum head.
$\alpha$ coefficient of bulk compressibility of the soil.
$\beta$ coefficient of bulk compressibility of the pore water.
$\delta t_{adapt}$ adaptive time step.
$\delta t_{base}$ base time step used when there is no time control.
$\delta_{ij}$ Kronecker delta function.
$\gamma$ unit weight of water.
$\kappa$ $T/S$.
$\Phi$ fluid potential.
$\rho$ density of water.
$\sigma'$ effective stress in the soil.
$\zeta_{soil}$ strain energy stored in a unit volume of the soil.
$\zeta_{water}$ strain energy stored in the pore water per unit bulk volume of soil.

*Acknowledgments.* The authors wish to thank the anonymous reviewers for their helpful comments. The computing support provided by the Department of Civil Engineering of the University of Toronto is acknowledged.

## REFERENCES

Bear, J., *Hydraulics of Groundwater, Ser. in Water Resour. and Environ. Eng.*, 569 pp., McGraw-Hill, New York, 1979.
Freeze, R. A., and A. J. Cherry, *Groundwater*, 604 pp., Prentice-Hall, Englewood Cliffs, N. J., 1979.
Gurtin, M. E., Variational principles for linear initial value problems, *Q. Appl. Math.*, *22*, 252–256, 1964.
Haberman, R., *Elementary Applied Partial Differential Equations With Fourier Series and Boundary Value Problems*, 2nd ed., 533 pp., Prentice-Hall, Englewood Cliffs, N. J., 1987.
Hubbert, K. M., Theory of groundwater motion, *J. Geol.*, *48*, 785–944, 1940.
Huyakorn, P. S., and G. F. Pinder, *Computational Methods in Subsurface Flow*, 473 pp., Academic, San Diego, Calif., 1983.
Jensen, O. K., An automatic time step selection scheme for reservoir simulation, paper presented at the 55th annual fall meeting of SPE-AIME, Soc. of Pet. Eng., Dallas, Tex., Sept. 21–24, 1980.
Karney, B. W., Energy methods in transient closed conduit flow, *J. Hydraul. Eng. Div. Am. Soc. Civ. Eng.*, *116*(10), 1180–1196, 1990.
Lindberg, B., Characterization of optimal step-size sequences for methods for stiff differential equations, *SIAM J. Numer. Anal.*, *14*, 859–887, 1977.
Mehra, R. K., M. Hadjitofi, and J. K. Donnelly, An automatic time step selector for reservoir models, paper presented at the 6th Symposium on Reservoir Simulation, Soc. of Pet. Eng., New Orleans, La., Feb. 1–3, 1982.
Pinder, G. F., and W. G. Gray, *Finite Element Simulation in Surface and Subsurface Hydrology*, 295 pp., Academic, San Diego, Calif., 1977.
Sammon, P. H., and B. Rubin, Practical control of time step selection in thermal simulation, paper presented at the 7th Symposium on Reservoir Simulation, Soc. of Pet. Eng., San Francisco, Calif., Nov. 15–18, 1983.
Wang, H. F., and M. P. Anderson, *Introduction to Groundwater Modelling: Finite Difference and Finite Element Methods*, 237 pp., W. H. Freeman, New York, 1982.
Yeh, W. W. G., *Groundwater Systems Planning and Management*, 416 pp., Prentice-Hall, Englewood Cliffs, N. J., 1987.

B. Karney, Department of Civil Engineering, University of Toronto, Toronto, Ontario, Canada M5S 1A4.
A. Seneviratne, Jacques Whitford Environment Limited, P. O. Box 1116, 711 Woodstock Road, Fredricton, New Brunswick, Canada E3B 5C2.

(Received July 9, 1990;
revised July 8, 1991;
accepted July 19, 1991.)